

1 *Unravelling vulture avoidance tactic of wind turbines*
2 *combining empirical and simulation data*

3

4 Sassi Yohan ^{1,*}, Ziletti Noémie ², Duriez Olivier ^{1,†}, Robira Benjamin ^{3,†}

5 1: CEFE, Univ Montpellier, CNRS, EPHE, IRD, Montpellier, France

6 2: LPO France site Grands Causses, Le Bourg, Peyreleau, France

7 3: Department of Biodiversity and Molecular Ecology, Research and Innovation Centre, Fondazione

8 Edmund Mach, San Michele all'Adige, Italy

9 * Corresponding author: yoh.sassi22@gmail.com, CEFE, 1919 Routes de Mende, 34293 Montpellier
10 cedex 5, France.

11 † These authors contributed equally.

12 Abstract

13 The increase of wind turbine installations to limit climate change may affect bird populations because
14 of collisions with rotor blades. Birds may respond to wind turbine presence along a gradient of
15 behavioural changes: avoiding the wind farm (macro-scale) or only the wind turbines either by
16 anticipating wind turbine locations (meso-scale) or engaging into last-minute flee attempts after late
17 perception (micro-scale). We investigated the flight response at these three spatial scales of 25 adult
18 griffon vultures (*Gyps fulvus*) equipped with GPS tags over three years when flying in an area including
19 ten wind farms in the Causses, France. At macro-scale, the population foraging range and habitat use
20 revealed that vultures did not avoid wind farms. To investigate avoidance at meso- and micro-scales we
21 focused on the four mostly visited wind farms. We compared vulture flights to null movement models,
22 based on a method allowing us to keep the correlation between flights and topography while creating
23 movement independent of wind turbine locations. At most sites, vultures did not show avoidance
24 behaviour. Yet, simulations from our agent-based model highlighted that the avoidance pattern detected
25 at one wind farm matched with an anticipated avoidance of turbines, probably linked to the presence of
26 a ridge nearby. Overall, our results suggest wind farm-specific responses by soaring birds as a function
27 of the landscape topography. Thus, stakeholders should carefully consider the wind farm location for
28 siting and designing preventive measures (e.g. improve detection of species not able to avoid turbines
29 in switching off on-demand technologies) to reduce collision risk of soaring birds.

30

31 **Key-words:** *Gyps fulvus*, renewable energy, collision risk, agent-based model, avoidance behaviour,
32 GPS telemetry

33 1. Introduction

34 Wind turbines are a solution to produce electricity with limited CO₂ emissions, although
35 their impact on wildlife raise some concerns about the large-scale deployment of this technology.
36 Meanwhile wind-power generation worldwide has grown dramatically during the last two decades (e.g.
37 by 70% from 2015 to 2019; IPCC, 2022), mortality due to collisions with the rotor blades have been
38 frequently reported in bats and birds (Schuster et al., 2015; Thaxter et al., 2017). Among birds, diurnal
39 raptors are considered as one of the most vulnerable taxa (Thaxter et al., 2017) because of their slow
40 pace of life which makes population viabilities particularly sensitive to additional adult mortality
41 (Bellebaum et al., 2013; Carrete et al., 2009; Dahl et al., 2012; Duriez et al., 2022).

42 In response to wind turbine occurrence, birds can develop avoidance mechanisms at three
43 spatial scales: macro-scale, meso-scale and micro-scale (May, 2015). Macro-scale avoidance refers to
44 an avoidance of the wind farm as a whole (e.g. in Cabrera-Cruz & Villegas-Patraca, 2016; Plonczkier
45 & Simms, 2012). Meso-scale avoidance describes an avoidance of the wind turbines several hundred to
46 thousands of metres ahead (e.g. in Garvin et al., 2011; Santos et al., 2022; Schaub et al., 2020). Micro-
47 scale avoidance stands for a last-second flee attempt of the rotor blades (typically < 200 m ahead) (May,
48 2015).

49 The avoidance tactic employed may be influenced by birds' perception abilities, but also and
50 largely by their morphology and flight capacities (Bevanger, 1998; Marques et al., 2014; Pennycuick,
51 2008). Several morphological parameters such as weight and wing area, which define wing loading,
52 have been identified as determinants for collision risks (Janss, 2000). Birds with high wing loading,
53 such as vultures and large eagles, have been shown to be more collision-prone than other raptors with
54 lower wing loading such as common buzzard (*Buteo buteo*) or short-toed eagles (*Circaetus gallicus*)
55 (Barrios & Rodríguez, 2004; de Lucas et al., 2008). The most likely reason for this pattern is that high
56 wing-loading influences flight type (Shepard, 2022) and is associated with lower flight manoeuvrability
57 (de Lucas et al., 2008). Unlike birds using flapping flight, large raptors use a soaring-gliding technique
58 based on thermal and orographic updrafts to gain altitude effortlessly (Duriez et al., 2014; Shepard,
59 2022). Thermal and orographic updrafts, which are respectively masses of hot rising air emanating from

60 heated surfaces and deviated wind onto topographical obstacles, constrain soaring birds in their
61 displacement (Pennycuick, 1998). Thus, landscape features can also play an important role in the
62 susceptibility of birds to collisions (de Lucas et al., 2012). While species with low wing loading could
63 easily avoid wind turbines a few metres ahead (Schaub et al., 2020), those with high wing loading such
64 as vultures will face much more difficulties. Despite being possible, a last minute flee attempt for large
65 soaring birds requires them to switch to flapping flight, a flight mode they can not hold for long because
66 of increased energetic costs (Duriez et al., 2014). Hence, if avoidance behaviour exists in these birds,
67 we could expect an anticipated avoidance (meso-scale) allowing them to glide to their next updraft.
68 This should particularly be true if the landscape favours thermal updraft or orographic uplift due to the
69 surrounding topography.

70 Up to now, studies on wind turbines avoidance behaviours focused mainly on medium-sized
71 birds with low wing loading such as black kites (*Milvus migrans*; Marques et al., 2020; Santos et al.,
72 2022) or Montagu's harrier (*Circus pygargus*; Schaub et al., 2020) which flight is relatively independent
73 of landscape features. In this study, we adapted new methods to study avoidance behaviour in griffon
74 vultures (*Gyps fulvus*), large soaring birds which depend largely on topography for their movements
75 (Scacco et al., 2023). We investigated whether vultures actively avoided wind farms (macro-scale
76 avoidance) and/or wind turbines (meso-/micro-scale avoidance). In the latter case, we aimed to
77 characterise what was the flight response to wind turbines (i.e. progressive long-distance avoidance or
78 last-minute flee attempt). Because of the dependence of their flight on the landscape, as well as their
79 low flight manoeuvrability, we expected vultures to prioritise long-distance anticipated avoidance of
80 wind turbines. Such in-depth investigations could particularly support stakeholder decisions by
81 providing applied knowledge on where to site wind farms and how far to detect birds to shut down wind
82 turbines in time to prevent collisions (McClure et al., 2021).

83 We used high-resolution GPS tracking of 25 adult individuals that ranged over 10 wind farms of
84 the Causses region, France, over three years. To investigate macro-scale avoidance, we estimated
85 vulture space utilisation distribution to determine whether vultures excluded wind farms from their
86 ranging area. We coupled this with a habitat selection analysis to estimate in-flight selection of wind
87 farms. To investigate meso- and micro-scale avoidance, we studied vulture movements within the four

88 most intensively used wind farms and compared them to a null model of expected movements if
89 independent of wind turbines location, obtained by rotating wind turbine locations. Furthermore, we
90 compared true flights within wind farms to those simulated with an agent-based model to have a
91 mechanistic understanding of the wind turbine avoidance manoeuvre (see Fig. 1 for framework).

92 2. Materials and methods

93 2.1. Study system

94 This study took place in the Causses region, France (Fig. 2), where a population of ca. 820
95 breeding pairs of griffon vultures live (census 2021, LPO). This region is characterised by limestone
96 plateaux interspersed by valleys. Valleys offer conditions for orographic updrafts that vultures can use
97 to soar efficiently. Away from the valleys, vultures patrol the open landscapes, relying on thermal
98 updrafts to gain height, looking for mortality in herds of grazing livestocks. In recent years, both the
99 number of vultures and the number of wind turbines have increased. There are nowadays 10 operating
100 wind farms (totalling 130 turbines) and nine additional are planned (projects totalling 91 turbines, Fig.
101 2), in a region where at least 30 vultures have been found dead due to collisions between 2012 and
102 2022 (including 10 casualties at the four focal wind farms cited below) (LPO/DREAL Occitanie,
103 unpublished). These wind farms are located between 18 km and 52 km from Cassagne, the geographical
104 centre of the breeding colony where a collective natural recycling station with vultures stands (44°12'N,
105 3°15'E, Fig. 2, Duriez et al., 2021).

106 We used tracking data spanning 3 years (from 1st January 2019 to 31st December 2021) from
107 25 vultures (Table S1) that had been captured in 2018 at Cassagne carcasses recycling station, and
108 equipped with 50 g solar-powered GPS-GSM tags (Ornittrack-50, Ornitela), in a leg-loop harness
109 configuration (Anderson et al., 2020). GPS tags were set to record location, speed and altitude at
110 intervals of 2-15 min depending on battery levels and season (generally lower battery levels in winter).
111 To study avoidance behaviour of operating wind turbines by vultures, we defined rectangular geofences
112 (virtual barriers) placed at 2 km from the most outlying turbines in each wind farm. Within these

113 geofences, GPS tags automatically shifted to high resolution recording (1 Hz) of individuals' location,
114 speed and altitude. This 2 km threshold was defined based on a compromise between the need of time
115 for the tags to switch to high resolution before entering the 1 km meso-scale buffer, and the need to
116 prevent battery discharge by recording at high resolution in areas that we were not interested in. To
117 retain only accurate in-flight GPS locations, we filtered the GPS locations of each individual by their
118 groundspeed (> 4 m/s) and their horizontal dilution of precision index (HDOP < 4) (Martin-Díaz et al.,
119 2020; Nathan et al., 2012). Data cleaning, processing and analysis were performed with *R* (version
120 4.2.2, R Core Team, 2022).

121 2.2 Data analysis

122 2.2.1. Macro-scale avoidance

123 To find out whether vultures expressed a macro-scale avoidance of wind farms, we computed
124 an in-flight utilisation distribution (UD) and an habitat selection function for each individual. First, we
125 resampled flights every 10 min to homogenise the sampling frequencies ("track_resample" function,
126 *amt* R package, Signer et al., 2019). Then, we focused on movements that were at a distance < 55 km
127 of the colony centre. This distance enabled the inclusion of all wind farms of the region while focusing
128 on vultures' daily flights (mean daily displacement from Cassagne by local birds equals 26 km (SD \pm
129 10 km), Fig. S1, Fluhr et al., 2021). Individuals' UD were estimated on these flights using brownian
130 random bridge-based kernels (Benhamou, 2011, *adehabitatHR* R package (Calenge, 2006), see
131 supplementary materials ESM01 for details). We then estimated a "population foraging range" as the
132 layering of the 95% isopleth of individual UD where each cell value corresponded to the number of
133 individual UD overlapping that cell (Duriez et al., 2019).

134 To estimate if vultures tended to fly further from wind turbines than expected by chance we
135 computed an habitat selection function (HSF; Fieberg et al., 2021). To do so, for each individual we
136 subsampled its daily datasets at three locations per day, evenly spaced during the main activity period
137 of vultures and not temporally autocorrelated (at 10:00, 12:00, 14:00; Fluhr et al., 2021). This allowed
138 us to categorise the locations "used" by individuals. In parallel, as the tracked vultures are central

139 place foragers (Monsarrat et al., 2013), we sampled 10-fold more locations following a bivariate
140 exponential distribution (“available locations”, Benhamou & Courbin, 2023). We restricted these
141 locations within a distance of 55 km from the colony centre. We fitted an HSF for each individual,
142 using the distance to the closest operational wind turbine as the only predictor. Each HSF corresponded
143 to a generalised linear mixed model with a binomial error structure (available: 0, used: 1) and a weighted
144 logit link function considering a weight of 5000 for available locations, and 1 for used locations. The
145 exponential of the unique slope estimate indicates whether vultures show no preference (≈ 1), favour
146 wind farms (> 1) or avoid wind farms (< 1) (Fieberg et al., 2021).

147 2.2.2 Meso- and micro-scale avoidance

148 To investigate meso- and micro-scale avoidance behaviour we focused on four wind farms: La
149 Baume, Montfreh, Mas de Naï and Saint Affrique. These wind farms were among the closest to the
150 centre of the vultures’ colony and were the most visited ones by vultures (Fig. 2, Table S2). Among the
151 25 vultures, 92% of them crossed at least once one of these four operating wind farms within the rotor
152 swept zone during the three years considered (Table S1).

153 2.2.2.1 Use of topography within wind farm geofences

154 In the geofenced areas of these winds farms, orographic updrafts are generated by steep slopes
155 associated to valleys, which are easily identifiable by a human eye in the coloured topography rasters
156 presented in Fig. 3 (Digital Elevation Model, IGN BDTOPO, 25 m resolution). Hence, we estimated
157 the central value of elevation among all pixels of the raster (i.e.
158 $\frac{\text{highest elevation value} + \text{lowest elevation value}}{2}$) and we created an isoline of elevation at this value. Then,
159 because orographic updrafts are generally drifted towards the upper part of the ridge we empirically
160 used a 300 m buffer to geographically define the area (hereafter called “slopes”) most likely to generate
161 orographic updrafts. To estimate how topography constrained vulture flight we computed another HSF.
162 Here we empirically found that subsampling 30% of the GPS locations composing each vulture track
163 in the considered geofenced area gave robust results while reducing autocorrelation between locations.
164 The locations “available” to vultures were randomly sampled within the geofenced area. The HSF used

165 to estimate the preference for slopes over other areas followed the same structure as mentioned above
166 with a dummy variable indicating whether the location was within a slope (1) or not (0) as a unique
167 predictor.

168 2.2.2.2 Wind farm rotation to create null model

169 To investigate whether vultures anticipated wind turbine locations to start manoeuvring at long
170 distance and/or whether they performed short-distance reflex manoeuvre to avoid them, we separated
171 flights for which vultures flew within the rotor-swept zone of wind turbines (i.e. between the minimum
172 rotor tip height and 15 m above the maximum rotor tip height, see Table S2 for wind farms' specific
173 values) and those for which vultures flew above the rotor-swept zone. These flights were rediscertised
174 at constant step length (50 m), to remove bias due to speed differences within and between the tracks
175 but also to reduce location aggregation due to circular soaring phases compared to rectilinear gliding
176 phases. Vultures can also fly below the rotor swept zone, yet, these events are rare (3.5 % of the
177 locations are below the rotor swept zone in our study), thus we did not consider that case.

178 We defined avoidance behaviour as a use of an area containing wind turbines lower than
179 expected if vulture flew independently of the wind turbine positions. To do so, we first estimated the
180 percentage of locations occurring within a given range of turbines (buffer zone) at their original positions
181 (e.g. 8.92% of the observed locations are within a 300 m buffer around wind turbines in the example
182 shown in Fig. 4A). Then we compared this observed percentage to a null distribution expected if
183 turbines were not avoided. We created this null distribution by recalculating the percentage of locations
184 included into the same buffer zone when the geofenced area containing the wind farm was rotated
185 around its barycenter from 10° to 350° with a 10° step (e.g. 12.33% of locations were included into the
186 300 m buffer with a 10° rotation in the example shown in Fig. 4B). Rotating the wind farm, instead of
187 the flight tracks, allowed us to preserve correlations between flights and topography, a necessary
188 condition for the null model to be biologically meaningful (Martin et al., 2008). This process, repeated
189 over buffers ranging from 50 to 1000 m from each turbine (with 50 m steps), provided a null distribution
190 associated with each buffer size.

191 For each buffer, we defined it as avoided when the observed proportion of locations was
192 significantly lower than expected through the null distribution. For this purpose, we ranked, by
193 increasing order, the 36 percentage values obtained for the considered buffer (the observed value, at
194 rotation = 0°, plus the 35 values from the rotations). We estimated the one-tailed probability (hereafter
195 p) by dividing the observed proportion rank by the total number of values (i.e. 36; Fig. 4C). A significant
196 avoidance of the buffer was detected ($p < 0.05$) when the observed percentage was ranked as the lowest
197 (i.e. $p = 1/36 = 0.028$). We applied this procedure for both flights within and above the rotor swept zone
198 separately. We checked that this rotation approach could adequately identify avoided buffers in each
199 wind farm when simulating different avoidance scenarii with our agent-based model described in the
200 following section (supplementary materials ESM02 and Fig. S2).

201 2.2.2.3 Agent-based model simulations

202 When a significant avoidance pattern was identified with the above-mentioned procedure, we
203 aimed at determining whether this pattern fitted with a long-distance anticipated avoidance or a last-
204 minute flee attempt. We built an agent-based model (DeAngelis & Mooij, 2005; Grimm & Railsback,
205 2005) simulating the behaviour of a virtual vulture able to perceive a turbine (and start manoeuvring)
206 at a distance d , and able to adjust its heading (known as turning angle) of α° every 5 m. This 5 m step
207 was meant to be as small as possible to mimic continuous movement, but sufficiently reasonable due to
208 computational limits. The environment, in which a virtual vulture flew, contained wind turbines whose
209 positions matched the true configuration of the studied wind farms.

210

211 Each simulation followed the subsequent flow:

- 212 1) A starting location was randomly selected on a side of the considered geofenced area and the
213 target location (reached only through strict ballistic movement) was defined on the mirroring
214 side, such that the target direction was θ .
- 215 2) The virtual vulture started moving in the direction of the target location, following a biased
216 random walk (Codling et al., 2008). This biased random walk consisted of movement steps of
217 5 m in the direction θ' sampled in a Von Mises distribution of mean θ (“rvm” function of the

218 *CircularDDM* package; Lin et al., 2018), and of persistence value κ (estimated based on the
219 true vulture tracks occurring at wind farms of comparison, redisccretised at a 5 m interval, using
220 the “est.kappa” function of the *CircStats* package, Lund & Agostinelli, 2018).

221 3) If the virtual vulture arrived at a defined distance of d metres from a wind turbine, it engaged
222 in an avoidance behaviour which consisted in maintaining a turning angle of α° opposite to the
223 turbine location (e. g. left if the turbine was initially located right with respect to the heading at
224 start of avoidance, and *vice versa*) at each step.

225 4) If the virtual vulture was avoiding a turbine, avoidance behaviour stopped as soon as the
226 distance to the turbine started to increase. It then resumed its biased random walk (heading to
227 the last direction after avoidance), and would return into avoidance behaviour whenever a new
228 turbine was perceived.

229 5) The simulation stopped when the agent flew out of the geofenced area.

230

231 We tested jointly for several values of α (0° to 14° by steps of 1° ; 14° representing the maximum
232 angle a griffon vulture can turn within a thermal; Williams et al., 2018) and d (50 m to 1000 m by a step
233 of 50 m, similar to the rotation procedure), repeating the simulations 10 000 for each set of parameters.
234 A small α and a large d would mimic long-distance anticipated avoidance, while a large α and a small
235 d would mimic last-minute flee attempt.

236 To understand the movements rules underpinning vultures’ avoidance behaviour, we focused
237 on buffer sizes detected as avoided, and compared the absolute fit of the simulations with the empirical
238 data. The absolute fit corresponded to the square of the difference between the percentage of locations
239 obtained by simulations and the one observed on empirical data (ϑ). In simulations mimicking
240 avoidance (d and $\alpha > 0$), we removed the ones for which the fit with empirical data was worse than for
241 cases with no avoidance ($\vartheta/\vartheta_{\text{null}} < 1$ where ϑ_{null} is the percent of location obtained in the buffer when
242 simulating no avoidance). For the remaining cases, we defined the fit quality between empirical and
243 simulated percentage of location with a buffer as $f = 1 - \vartheta/\vartheta_{\text{null}}$. A perfect fit (i.e. the combination of α

244 and d that correctly mimicked the observed vulture avoidance behaviour in the considered buffer) would
245 give $f = 1$.

246 **3. Results**

247 **3.1 Avoidance behaviour of wind farms at macro-scale**

248 The population foraging range overlapped with 100% of the wind farm projects and 60% of the
249 operating wind farms (Fig. 2). The turbines of the furthest wind farm from the colony centre, Mas de
250 Naï, was included into the in-flight utilisation range of five vultures while one of the closest wind farm,
251 La Baume, cut off the airspace used by 18 individuals (Fig. 2). In addition, the mean exponential of the
252 HSF estimate associated with the closest distance to operational wind turbines was extremely close to
253 1 ($0.99 \pm \text{SD } 4.82 \times 10^{-5}$) suggesting no preferences toward large distances from wind turbines.

254 **3.2 Avoidance behaviour of wind turbines at meso-/micro-scale**

255 **3.2.1 Importance of the topography when flying in the wind farms**

256 Vultures crossed the wind farms several times during these three years (all individuals pooled,
257 [min,max] = [207, 1793] in Montfreh and La Baume, respectively - Table S1 and S2). The proportions
258 of tracks that entered the rotor swept zone of these wind farms were not negligible ([min,max] =
259 [32.84%, 50.28%] in Montfreh and Mas de Naï, respectively).

260 In the area defined by the geofences, 15.3% of La Baume, 51.5% of Montfreh, 80.5% of Mas
261 de Naï and 19.7% of Saint Affrique, were represented by slopes (Fig. 3). While flying in these areas,
262 vultures significantly favoured these slopes (exponential of HSF estimate associated to slope use [95%
263 confidence interval]; La Baume: 1.807 [1.767,1.848], $p < 0.001$; Montfreh: 1.193 [1.106,1.287], $p <$
264 0.001; Mas de Naï: 1.306 [1.246,1.370], $p < 0.001$; Saint Affrique: 1.143 [1.088,1.200], $p < 0.001$).

265 **3.2.2 Detection of active avoidance of wind turbines**

266 In three wind farms (La Baume, Mas de Naï, and Saint Affrique), no avoidance behaviour was
267 detected either for flights above or within the rotor swept zone (Fig. S3). In Montfreh, we did not

268 detect avoidance when focusing on flights above the rotor swept zone (Fig. 5A). However, for flights
269 within this risky zone, we observed a significantly lower proportion of GPS locations than expected for
270 buffers from 50 m to 450 m (Fig. 5B). This suggests a significant avoidance in this range of distances,
271 matching with the availability of steep slopes nearby (Fig. 5C).

272 3.2.3 Characterisation of meso- and micro-scale avoidance tactic

273 We further scrutinised flights in Montfreh, by comparing the amount of vulture locations
274 observed within buffers around wind turbines, where avoidance was detected, to the amount obtained
275 with agent-based simulations. Simulations with large distances of detection and low turning angles
276 yielded best matches with observations for most of the buffers highlighting a predominant long-distance
277 avoidance tactic (Fig. 5D). However, for the smallest buffers the best fit ($f > 0.95$) between simulated
278 and observed data could be obtained for both low and large turning angle values, suggesting potential
279 last-minute flee attempts (e.g. the observed avoidance of the 200 m buffer is well simulated with both
280 sets of parameters: $d = 500$ m with $\alpha = 1^\circ$ and $d = 250$ m with $\alpha = 6^\circ$, Fig. 5D).

281 4. Discussion

282 Combining high-resolution GPS tracking data from 25 adult griffon vultures across four
283 wind farms and simulations from an agent-based model revealed that wind turbine avoidance seems
284 relatively limited in this species, possibly with specific responses in each wind farm strongly associated
285 with landscape topography. The landscape surrounding wind farms thus appears of prime importance
286 and should thus prevail for deciding wind farm siting.

287 Our exploration of the population foraging range coupled with the habitat selection analysis
288 highlighted that wind farm areas were still exploited by vultures. Precisely, we demonstrated that griffon
289 vultures did not exhibit a macro-scale avoidance of the wind farms. This reminds of former results on
290 other large raptors such as white-tailed eagles (*Haliaeetus albicilla*; Dahl et al., 2013) but contradicts
291 results of macro-scale avoidance in medium-size birds such as migrating raptors at onshore wind farms

292 (Cabrera-Cruz & Villegas-Patraca, 2016) and aquatic birds at offshore wind farms (e.g. in Plonczkier
293 & Simms, 2012).

294 At meso-scale, we observed signs of avoidance behaviour, up to 450 m, only at one wind
295 farm (Montfreh) among four commonly crossed by vultures. Unlike other wind farms, Montfreh
296 turbines were located at about 500 m from steep slopes that were significantly selected by vultures for
297 their foraging and commuting movements. Such a site-specific response could be explained by the
298 topography of Montfreh, where vultures could reach slopes to take advantage of orographic uplift and
299 fly parallel to the row of turbines (like black kites in Santos et al., 2022). Since it only requires
300 positioning themselves over windward slopes to benefit from the deviated wind above canyons' ridges
301 and slopes, the predictability of orographic updrafts make them easier to exploit compared to thermals
302 (Katzner et al., 2012; Shepard, 2022). As such, the avoidance of wind turbines identified by our analyses
303 could be "passive", as a by-product of topography, rather than an active avoidance due to a perceived
304 threat. Indeed, as the strength of the slope uplift decreases with height above ground level (Shepard,
305 2022), vultures flying above 200 m over ground would no longer be able to rely on this source of uplift
306 (Duerr et al., 2019). This framed consistently with the lack of avoidance when considering flights above
307 the rotor swept zone at all wind farms, including Montfreh.

308 Far away from used slopes and ridges, as in the three remaining wind farms where we did not
309 detect any avoidance, soaring birds may rely almost exclusively on thermals to gain altitude (Katzner
310 et al., 2012). Péron et al. (2017) estimated that the probability for griffon vultures and other large raptors
311 to fly above 200 m (i.e. above the rotor-swept zone) was significantly correlated to thermal uplift
312 potential. Being constrained in their movements by such unpredictable resources may explain why
313 soaring bird mortality by collision on wind turbines increases when thermals are less frequent or less
314 powerful (e.g. during rainfall or during winter; Barrios & Rodríguez, 2004; Marques et al., 2014). The
315 circling flight necessary to rise into thermal may be associated with a higher risk of collision than when
316 using (linear) slope soaring due to repeated passages in the same area at increasing altitudes (Barrios &
317 Rodríguez, 2004). This may also explain why many bird species that rely on the same flight tactics
318 suffer heavy losses by collisions (Barrios & Rodríguez, 2004; de Lucas et al., 2008; Heuck et al., 2019;
319 Katzner et al., 2012) and concur with a fairly low support for a last-minute flee attempt in our analyses.

320 Such last-minute avoidance should require sharp turns, which are better achieved by birds with low
321 wing-loading and elongated tails, which is not the case of *Gyps* vultures that possess a rather short tail
322 and high wing loading (Balmford, 1995; Gillies et al., 2011). Such manoeuvre could still occur in rare
323 cases of emergency but would result in a very rapid loss of altitude for the vultures. This picture,
324 however, contrasts partially with recent evidence on black kites and Montagu's harriers showing that
325 flight behaviour was modified at a close range of wind turbines suggesting an active avoidance in these
326 species (Santos et al., 2022; Schaub et al., 2020). These species, having a lower wind loading, are
327 probably much less constrained by sources of uplift in their movements, giving them more room to
328 adapt their flights according to perceived risks, likely explaining the observed differences in avoidance
329 behaviour.

330 In this study we adapted a method consisting of rotating the locations of infrastructure to be
331 avoided (here wind turbines) to construct null models distributions of space use independent of
332 infrastructure locations. This method is similar in principle to the usual method to rotate tracks to create
333 a null model (e.g. in Schaub et al., 2020) but it has the double advantage of saving the correlation
334 between topography and animal flight, and also reducing the computation power (and time) needed to
335 perform rotations of large amounts of tracks. This is particularly valuable for species heavily relying on
336 topography to move through landscapes, whose rotated flight would become biologically unrealistic. In
337 addition, the use of an agent-based model allowed us to highlight the robustness of our method and be
338 confident in the pattern detected on empirical data. It is also a practical approach for understanding the
339 processes underlying animal movements (Tang & Bennett, 2010), but is often overlooked for analysing
340 collision and turbine avoidance by flying animals (but see in birds: Eichhorn et al., 2012, in bats:
341 Ferreira et al., 2015). We have provided here a model that can be used as a framework for further
342 investigation of the risk of collision with wind turbines. All together, our results revealed a new level
343 of complexity in wind turbine avoidance behaviours as even among restricted groups such as soaring
344 raptors, answer to turbine presence seem to be species- and site-specific.

345 5. Conclusion and management implications

346 The tragic conflict that we currently face is that soaring birds and wind energy developers are
347 targeting the same resource: wind. The development of wind farms pose a major conservation problem
348 for most large flying animals (Thaxter et al., 2017), as they can induce disturbance of the environment,
349 leading to a decrease in local biodiversity, and can also lead to disruptions of population dynamics and
350 stability through collision fatalities (Perrow, 2017). Here, we provided further evidence that the flight
351 capabilities of some species may make them particularly sensitive to wind turbine collisions, and do not
352 allow them to avoid wind turbines effectively. Yet, we detected an anticipated avoidance at one wind
353 farm matching with the presence of slopes. Slopes aggregate soaring birds and may allow them to stay
354 away from turbines, provided they are neither too close (high risk of collision using the slope uplift)
355 nor too far away (high risk of collision using only thermal uplift; Péron et al., 2017). Taking into account
356 distance from turbines to favourable conditions when siting projects could help to reduce collision risk.
357 However this would require further research to first understand what makes some slopes more attractive
358 to soaring birds, as all slopes are not necessarily used. Furthermore, it would imply a better
359 understanding of the distance which would be optimal to reduce collision risk. At already operating
360 sites it has become crucial to detect birds unable to avoid turbines well in advance to shutdown turbines
361 in time to prevent collisions. Shutdown on-demand when animals at risk are detected is a potentially
362 promising way to reduce collision mortality with a negligible reduction in energy production, yet
363 automatic detection systems are costly and their efficiency is still debated (McClure et al., 2021; Tomé
364 et al., 2017). Straightforwardly, to solve this green-green dilemma to reduce carbon emission and
365 preserve biodiversity, it would be more efficient, and should be prioritised, to prevent siting the turbines
366 at places where soaring birds are obliged to travel.

367 CRediT authorship contribution statement

368 **Yohan Sassi**: Conceptualization, Methodology, Software, Formal analysis, Visualisation, Writing -
369 Original Draft, Writing - Review & Editing. **Noémie Ziletti**: Conceptualization, Funding acquisition,
370 Writing - Review & Editing. **Olivier Duriez**: Conceptualization, Data curation, Visualisation, Writing
371 - Review & Editing, Supervision. **Benjamin Robira**: Conceptualization, Methodology, Software,
372 Formal analysis, Visualisation, Writing - Original Draft, Writing - Review & Editing, Supervision.

373 Declaration of competing interest

374 The authors declare to have no conflict of interest

375 Data availability

376 GPS telemetry data are stored in the www.movebank.org database in the study “Eurasian Griffon
377 vulture in France (Grands Causses 2018) ID_PROG 961”. Given the sensitive nature of tracking data
378 for protected species, downloading permission should be asked through the platform to OD. Scripts
379 for review are available here: <https://github.com/YohanSassi/windTurbinesAvoidance>. A perennial
380 storage will be provided after revision (e.g. Zenodo).

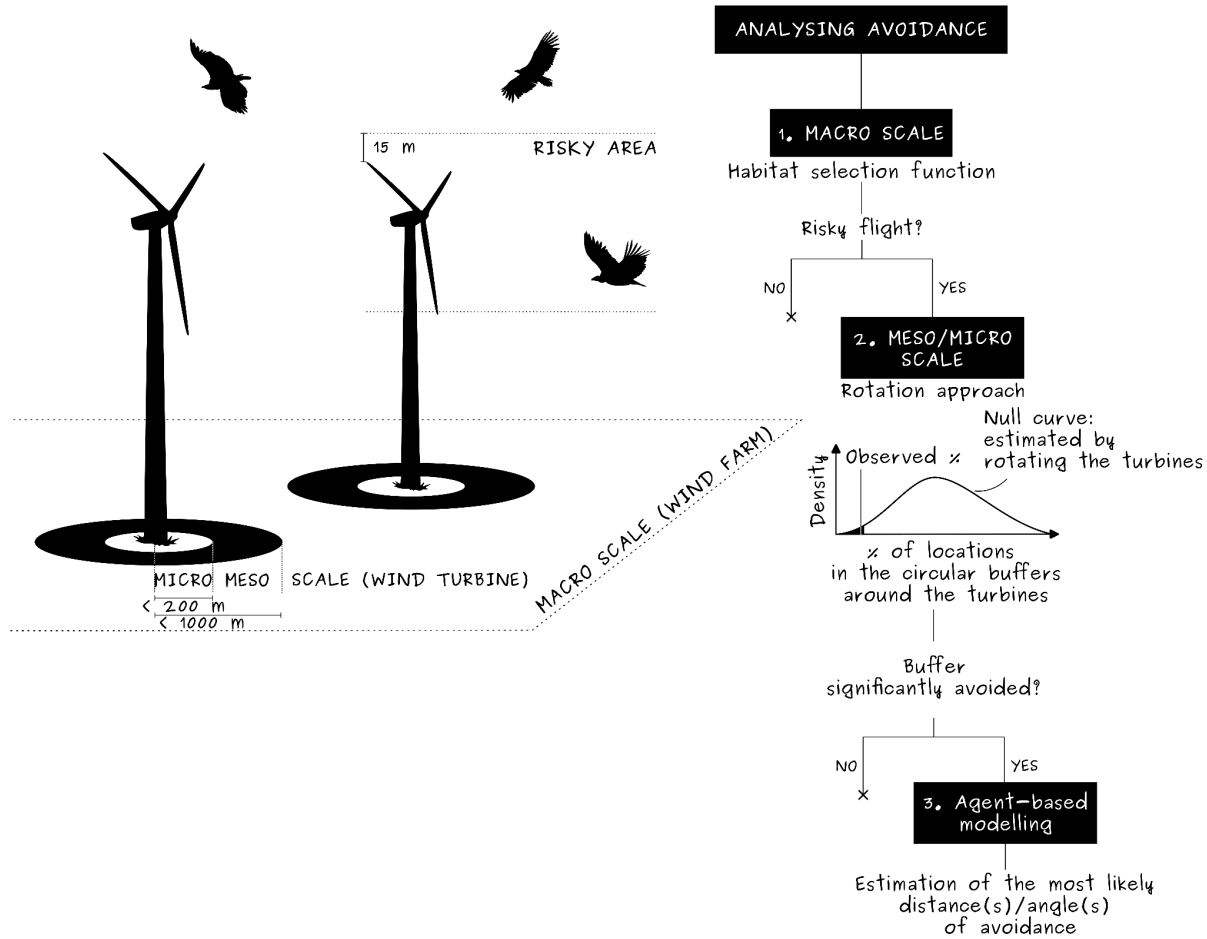
381 Acknowledgment

382 We thank the staff from the Grands Causses site of LPO France (T David, R Straughan, R Nadal L
383 Giraud, P Lecuyer, B Descaves) for helping in capturing vultures for tagging. Telemetry study of
384 vultures was authorised in the Programme Personnel 961, coordinated by O. Duriez, under the
385 supervision of the French ringing centre, CRBPO, Paris. We also thank Patrick Boudarel (DREAL
386 Occitanie, France) for fatalities data in the Occitanie region, France and Simon Benhamou for helpful
387 discussions regarding data analyses.

388 Fundings

389 This work was supported by the GAIA doctoral school grant, University of Montpellier (YS), the
390 Gordon and Betty Moore Foundation (BR). GPS tags were purchased with funds from the European
391 Regional Development (2014-2020) "Conservation des rapaces nécrophages des milieux ouverts
392 herbacés du Massif central" (NZ).

393 Main text figures

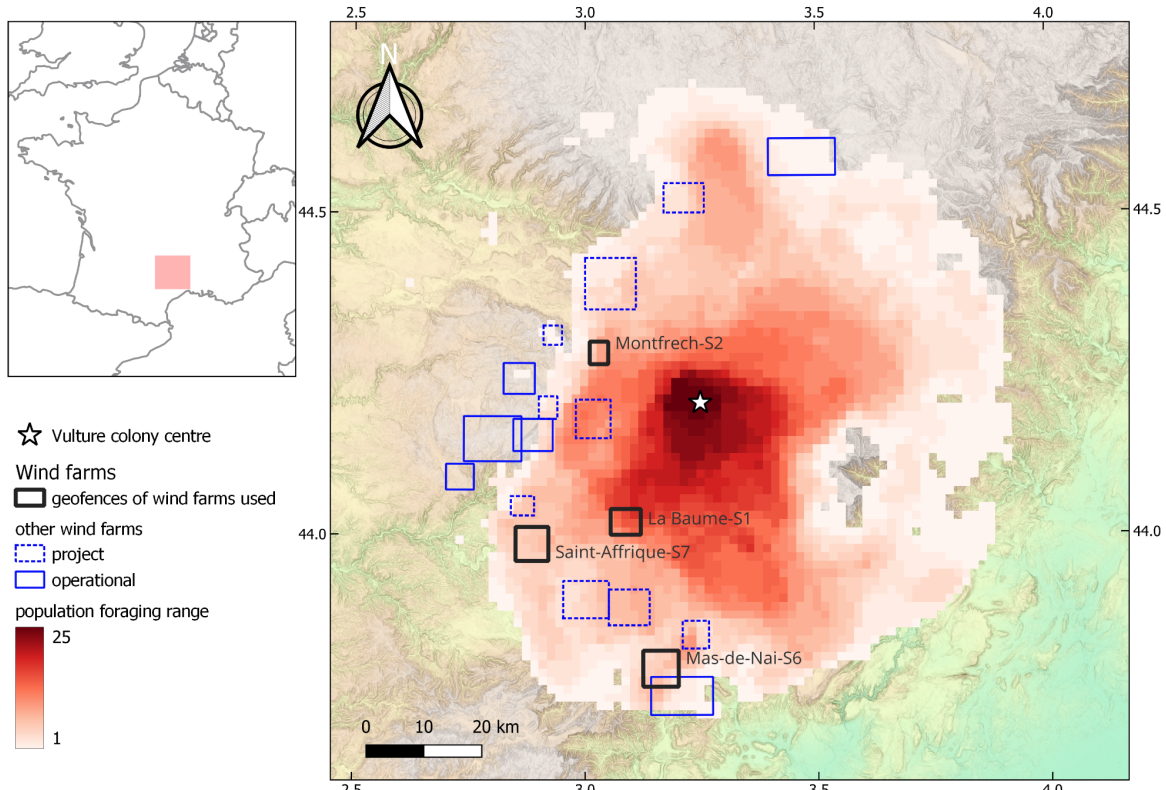


394

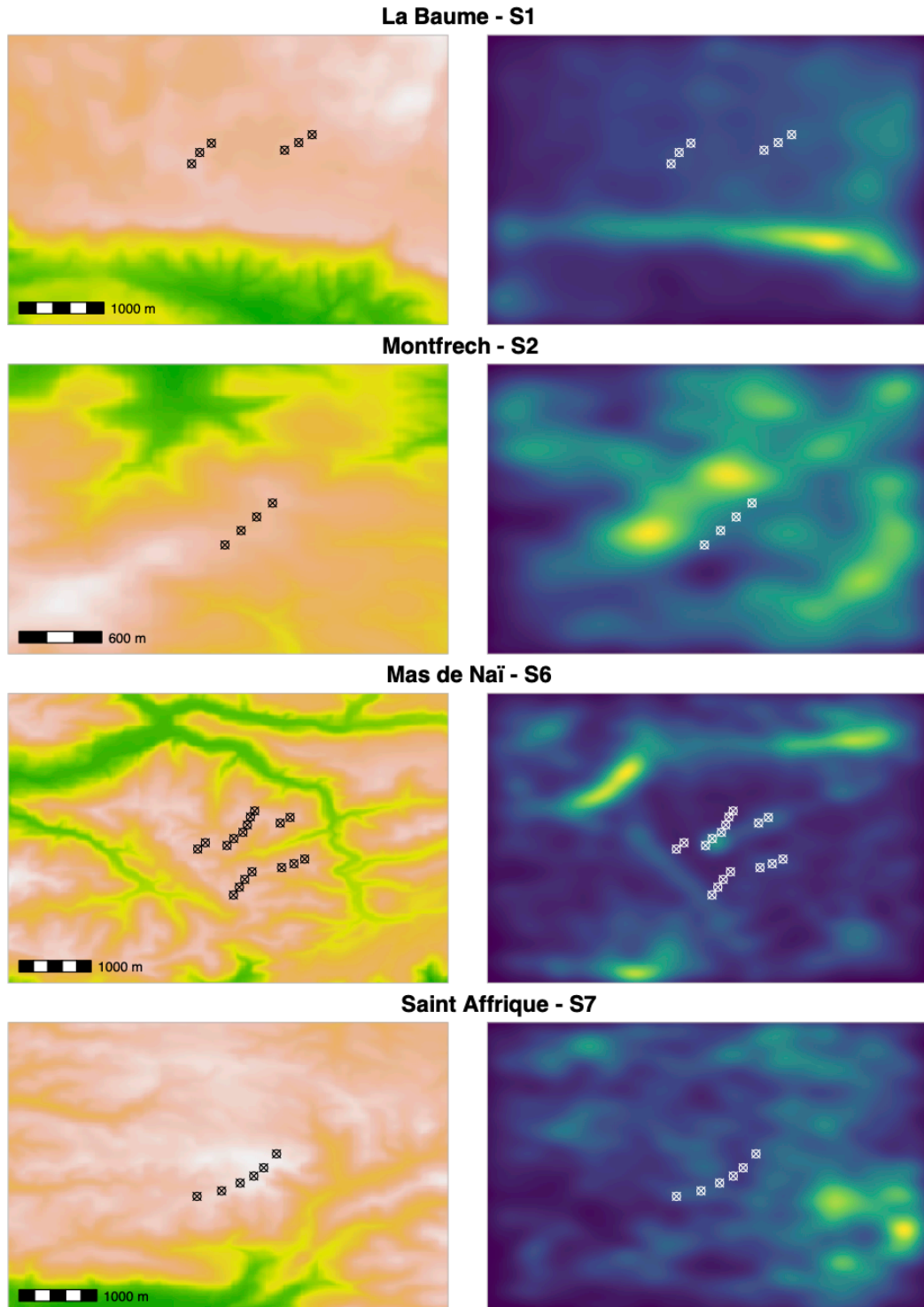
395 **Fig. 1. Illustration of the methodological framework used to investigate wind turbine avoidance**

396 **in vultures.** Avoidance tactics were studied at the macro scale (avoidance of the entire wind farm) or
397 at the micro/meso scale (avoidance of wind turbines, from a hundred to a thousand metres) (left). We
398 used a top-down approach from the largest to the smallest scale (right) combining empirical and
399 simulation data.

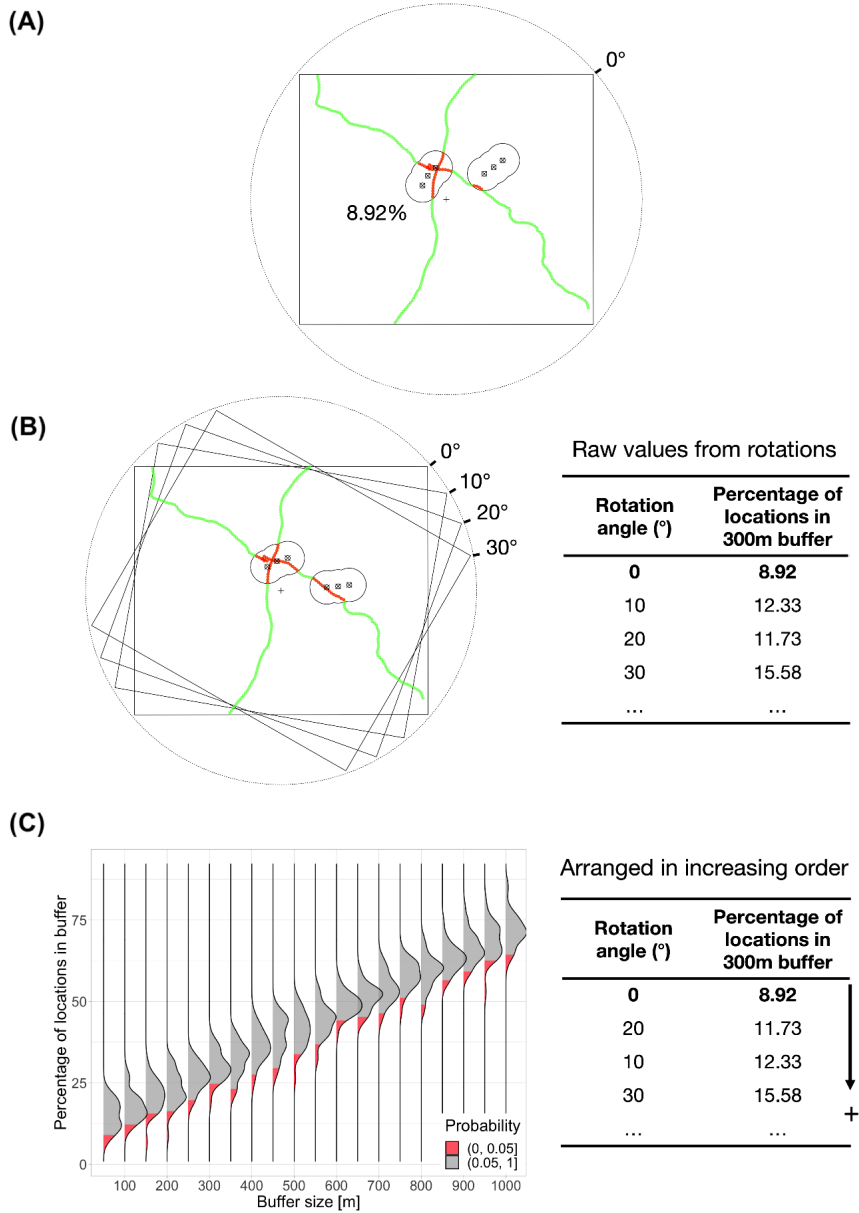
400



401
402 **Fig. 2. Global vulture population foraging range in the Causses region, France.** The darker the
403 colour of the red raster, the higher the number of individual in-flight 95% utilisation distributions that
404 overlap the given cell. Additional rectangles represent geofences around wind farms (black: study wind
405 farms, plain blue: operational wind farms; dotted blue: project of construction). The star is the
406 geographical centre of the nesting colony, Cassagne, where vultures have been reintroduced, are tagged
407 and where a carcasse recycling station is located.



408 **Fig. 3. Topography and vulture space utilisation distribution in the studied wind farms.**
409 Topography distribution (left column; green to white gradient indicating increasing altitude) and the
410 weighted mean utilisation distribution (right column, blue to green gradient indicating increasing use
411 intensity). See supplementary materials ESM01 for details on the estimation of the mean utilisation
412 distribution.

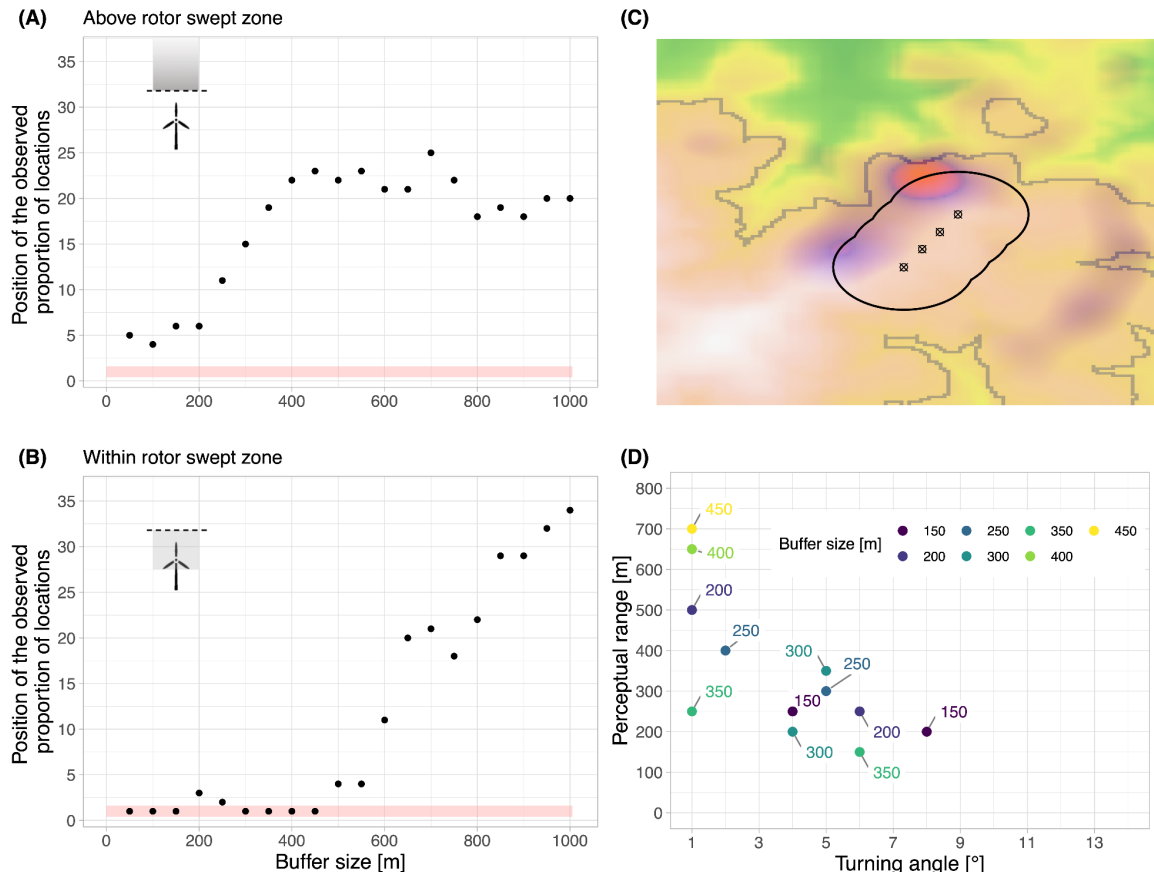


With 36 rotations, one tailed p-value is significant only if the observed percentage of locations in the buffer is the lowest (i.e. ranked first when ordering values in increasing order) :

$$p = \frac{\text{rank of the observed percentage}}{\text{number of rotations (i.e. 36)}}$$

413 **Fig. 4. Visual guide of the rotational approach used to estimate vulture turbine avoidance. (A)**
414 The geofence is represented by the rectangle around the wind farm (e.g. La Baume here). Wind turbines
415 are indicated by the crossed circles and are surrounded by a specific buffer zone (e.g. 300 m here), the
416 merged limits of which are shown by the solid black line. Two vulture flights are represented by the
417 green and red lines (outside or inside buffers, respectively). For the original (true) wind turbine positions
418 (0° of rotation), the percentage of vulture locations observed in the buffer was estimated. (B) A null
419 model was constructed by rotating the wind turbines around the wind farm barycentre from 10° to 350°

420 by steps of 10°. For each rotation the percentage of vulture locations in the considered buffer was
421 calculated, giving 36 values of percentage per buffer size (1 observed and 35 theoretical values). (C)
422 This method was applied to buffers from 50 m to 1000 m by steps of 50 m around wind turbines,
423 providing a null distribution of expected percentage for each buffer size. An avoidance should be
424 detected if the truly observed percentage of locations in the buffer (i.e. for rotation angle = 0°) fell into
425 the red part of the distribution. Hence, for each buffer size the percentages of locations were ranked by
426 increasing order and we estimated the one-tailed p-value by dividing the rank of the truly observed
427 percentage in the arranged distribution by the total number of rotations. Thus, the observed percentage
428 of locations in the buffer was significantly lower than expected if it was ranked first in the distribution:
429 $p = 1/36 = 0.028$. (These are simulated data for illustration)



430 **Fig. 5. Turbines avoidance in Montfrehc wind farm.** Results of the rotation analysis conducted on
 431 vultures' flights above (A) and within (B) the rotor swept zone: dots represent the position of the
 432 observed percentage of location, among the 36 estimated values (y-axis) during the rotational analysis,
 433 within a given circular buffer around wind turbines (x-axis). The red rectangle highlights buffers for
 434 which the amount of locations observed is significantly lower than randomly expected. (C) illustrates
 435 the overlap between topography (green to white gradient indicating increasing altitude) and utilisation
 436 distribution (purple to red gradient indicating increasing use intensity) of the Montfrehc wind farm. The
 437 solid black line represents the limits of merged 450-m buffers around wind turbines. (D) shows the
 438 combination of parameters (perceptual range and turning angle) used in the agent-based model to
 439 simulate vulture flights yielding the best fits between simulations and observations ($f > 0.95$).

440 References

441 Anderson, D., Arkumarev, V., Bildstein, K., Botha, A., Bowden, C., Davies, M., Duriez, O.,
442 Forbes, N. A., Godino, A., Green, R., Krüger, S., Lambertucci, S. A., Orr-Ewing, D.,
443 Parish, C. N., Parry-Jones, J., & Weston, E. (2020). *A practical guide to methods for*
444 *attaching research devices to vultures and condors.*
445 <https://doi.org/10.17863/CAM.58032>

446 Balmford, A. (1995). How Natural Selection Shapes Birds' Tails. *The American Naturalist*,
447 146(6), 848–868. <https://doi.org/10.1086/285828>

448 Barrios, L., & Rodríguez, A. (2004). Behavioural and environmental correlates of soaring-bird
449 mortality at on-shore wind turbines. *Journal of Applied Ecology*, 41(1), 72–81.
450 <https://doi.org/10.1111/j.1365-2664.2004.00876.x>

451 Bellebaum, J., Korner-Nievergelt, F., Dürr, T., & Mammen, U. (2013). Wind turbine fatalities
452 approach a level of concern in a raptor population. *Journal for Nature Conservation*,
453 21(6), 394–400. <https://doi.org/10.1016/j.jnc.2013.06.001>

454 Benhamou, S. (2011). Dynamic Approach to Space and Habitat Use Based on Biased
455 Random Bridges. *PLOS ONE*, 6(1), e14592.
456 <https://doi.org/10.1371/journal.pone.0014592>

457 Benhamou, S., & Courbin, N. (2023). Accounting for central place foraging constraints in
458 habitat selection studies. *Ecology*, e4134. <https://doi.org/10.1002/ecy.4134>

459 Bevanger, K. (1998). Biological and conservation aspects of bird mortality caused by
460 electricity power lines: A review. *Biological Conservation*, 86(1), 67–76.
461 [https://doi.org/10.1016/S0006-3207\(97\)00176-6](https://doi.org/10.1016/S0006-3207(97)00176-6)

462 Cabrera-Cruz, S. A., & Villegas-Patraca, R. (2016). Response of migrating raptors to an
463 increasing number of wind farms. *Journal of Applied Ecology*, 53(6), 1667–1675.
464 <https://doi.org/10.1111/1365-2664.12673>

465 Calenge, C. (2006). The package “adehabitat” for the R software: A tool for the analysis of
466 space and habitat use by animals. *Ecological Modelling*, 197(3), 516–519.

467 <https://doi.org/10.1016/j.ecolmodel.2006.03.017>

468 Carrete, M., Sánchez-Zapata, J. A., Benítez, J. R., Lobón, M., & Donázar, J. A. (2009).

469 Large scale risk-assessment of wind-farms on population viability of a globally

470 endangered long-lived raptor. *Biological Conservation*, 142(12), 2954–2961.

471 <https://doi.org/10.1016/j.biocon.2009.07.027>

472 Codling, E. A., Plank, M. J., & Benhamou, S. (2008). Random walk models in biology.

473 *Journal of The Royal Society Interface*, 5(25), 813–834.

474 <https://doi.org/10.1098/rsif.2008.0014>

475 Dahl, E. L., Bevanger, K., Nygård, T., Røskift, E., & Stokke, B. G. (2012). Reduced breeding

476 success in white-tailed eagles at Smøla windfarm, western Norway, is caused by

477 mortality and displacement. *Biological Conservation*, 145(1), 79–85.

478 <https://doi.org/10.1016/j.biocon.2011.10.012>

479 Dahl, E. L., May, R., Hoel, P. L., Bevanger, K., Pedersen, H. C., Røskift, E., & Stokke, B. G.

480 (2013). White-tailed eagles (*Haliaeetus albicilla*) at the Smøla wind-power plant,

481 Central Norway, lack behavioral flight responses to wind turbines. *Wildlife Society*

482 *Bulletin*, 37(1), 66–74. <https://doi.org/10.1002/wsb.258>

483 de Lucas, M., Ferrer, M., & Janss, G. F. E. (2012). Using Wind Tunnels to Predict Bird

484 Mortality in Wind Farms: The Case of Griffon Vultures. *PLoS ONE*, 7(11), e48092.

485 <https://doi.org/10.1371/journal.pone.0048092>

486 de Lucas, M., Janss, G. F. E., Whitfield, D. P., & Ferrer, M. (2008). Collision fatality of

487 raptors in wind farms does not depend on raptor abundance. *Journal of Applied*

488 *Ecology*, 45(6), 1695–1703. <https://doi.org/10.1111/j.1365-2664.2008.01549.x>

489 DeAngelis, D. L., & Mooij, W. M. (2005). Individual-based modeling of ecological and

490 evolutionary processes. *Annual Review of Ecology, Evolution, and Systematics*, 36,

491 147–168.

492 Duerr, A. E., Miller, T. A., Dunn, L., Bell, D. A., Bloom, P. H., Fisher, R. N., Tracey, J. A., &

493 Katzner, T. E. (2019). Topographic drivers of flight altitude over large spatial and

494 temporal scales. *The Auk*, 136(2), ukz002. <https://doi.org/10.1093/auk/ukz002>

495 Duriez, O., Andevski, J., Bowden, C. G. R., Camiña-Cardenal, A., Frey, H., Genero, F.,
496 Hatzofe, O., Llopis-Dell, A., Néouze, R., Phipps, L., & Tavares, J. (2021).
497 Commentary: Not All Vulture Feeding Stations are Supplementary—Proposed
498 Terminology for Carcass Provisioning with Reference to Management Goals and
499 Food Sources. *Journal of Raptor Research*, 56(1), 131–137.
500 <https://doi.org/10.3356/JRR-20-19>

501 Duriez, O., Descaves, S., Gallais, R., Neouze, R., Fluhr, J., & Decante, F. (2019). Vultures
502 attacking livestock: A problem of vulture behavioural change or farmers' perception?
503 *Bird Conservation International*, 29(3), 437–453.
504 <https://doi.org/10.1017/S0959270918000345>

505 Duriez, O., Kato, A., Tromp, C., Dell'Omo, G., Vyssotski, A. L., Sarrazin, F., & Ropert-
506 Coudert, Y. (2014). How Cheap Is Soaring Flight in Raptors? A Preliminary
507 Investigation in Freely-Flying Vultures. *PLoS ONE*, 9(1), e84887.
508 <https://doi.org/10.1371/journal.pone.0084887>

509 Duriez, O., Pilard, P., Saulnier, N., Boudarel, P., & Besnard, A. (2022). Windfarm collisions
510 in medium-sized raptors: Even increasing populations can suffer strong demographic
511 impacts. *Animal Conservation*, n/a(n/a). <https://doi.org/10.1111/acv.12818>

512 Eichhorn, M., Johst, K., Seppelt, R., & Drechsler, M. (2012). Model-Based Estimation of
513 Collision Risks of Predatory Birds with Wind Turbines. *Ecology and Society*, 17(2),
514 art1. <https://doi.org/10.5751/ES-04594-170201>

515 Ferreira, D., Freixo, C., Cabral, J. A., Santos, R., & Santos, M. (2015). Do habitat
516 characteristics determine mortality risk for bats at wind farms? Modelling susceptible
517 species activity patterns and anticipating possible mortality events. *Ecological
518 Informatics*, 28, 7–18. <https://doi.org/10.1016/j.ecoinf.2015.04.001>

519 Fieberg, J., Signer, J., Smith, B., & Avgar, T. (2021). A 'How to' guide for interpreting
520 parameters in habitat-selection analyses. *Journal of Animal Ecology*, 90(5), 1027–
521 1043. <https://doi.org/10.1111/1365-2656.13441>

522 Fluhr, J., Benhamou, S., Peyrusque, D., & Duriez, O. (2021). Space Use and Time Budget in

523 Two Populations of Griffon Vultures in Contrasting Landscapes. *Journal of Raptor*
524 *Research*, 55(3), 425–437. <https://doi.org/10.3356/JRR-20-14>

525 Garvin, J. C., Jennelle, C. S., Drake, D., & Grodsky, S. M. (2011). Response of raptors to a
526 windfarm. *Journal of Applied Ecology*, 48(1), 199–209. <https://doi.org/10.1111/j.1365->
527 2664.2010.01912.x

528 Gillies, J. A., Thomas, A. L. R., & Taylor, G. K. (2011). Soaring and manoeuvring flight of a
529 steppe eagle *Aquila nipalensis*. *Journal of Avian Biology*, 42(5), 377–386.
530 <https://doi.org/10.1111/j.1600-048X.2011.05105.x>

531 Grimm, V., & Railsback, S. (2005). *Individual-based Modeling and Ecology* (Princeton
532 university press.).
533 <https://press.princeton.edu/books/paperback/9780691096667/individual-based->
534 modeling-and-ecology

535 Harel, R., Duriez, O., Spiegel, O., Fluhr, J., Horvitz, N., Getz, W. M., Bouten, W., Sarrazin,
536 F., Hatzofe, O., & Nathan, R. (2016). Decision-making by a soaring bird: Time,
537 energy and risk considerations at different spatio-temporal scales. *Philosophical
538 Transactions of the Royal Society B: Biological Sciences*, 371(1704), 20150397.
539 <https://doi.org/10.1098/rstb.2015.0397>

540 Heuck, C., Herrmann, C., Levers, C., Leitão, P. J., Krone, O., Brandl, R., & Albrecht, J.
541 (2019). Wind turbines in high quality habitat cause disproportionate increases in
542 collision mortality of the white-tailed eagle. *Biological Conservation*, 236, 44–51.
543 <https://doi.org/10.1016/j.biocon.2019.05.018>

544 Hull, C. L., & Muir, S. C. (2013). Behavior and turbine avoidance rates of eagles at two wind
545 farms in Tasmania, Australia. *Wildlife Society Bulletin*, 37(1), 49–58.
546 <https://doi.org/10.1002/wsb.254>

547 IPCC. (2022). *Technical Summary. In: Climate Change 2022: Mitigation of Climate Change.*
548 *Contribution of Working Group III to the Sixth Assessment Report of the
549 Intergovernmental Panel on Climate Change.* <https://www.ipcc.ch/report/ar6/wg3/>

550 Janss, G. F. E. (2000). Avian mortality from power lines: A morphologic approach of a

551 species-specific mortality. *Biological Conservation*, 95(3), 353–359.

552 [https://doi.org/10.1016/S0006-3207\(00\)00021-5](https://doi.org/10.1016/S0006-3207(00)00021-5)

553 Katzner, T. E., Brandes, D., Miller, T., Lanzone, M., Maisonneuve, C., Tremblay, J. A.,

554 Mulvihill, R., & Merovich Jr, G. T. (2012). Topography drives migratory flight altitude

555 of golden eagles: Implications for on-shore wind energy development. *Journal of*

556 *Applied Ecology*, 49(5), 1178–1186. <https://doi.org/10.1111/j.1365-2664.2012.02185.x>

558 Lin, Y.-S., Heathcote, A., & Kvam, P. (2018). *CircularDDM: Circular Drift-Diffusion Model*. *R*

559 *package version 0.1.0*. [Computer software]. <https://CRAN.R-project.org/package=CircularDDM>

561 Lund, U., & Agostinelli, C. (2018). *CircStats: Circular Statistics, from 'Topics in Circular*

562 *Statistics'* (R package version 0.2-6) [Computer software]. <https://CRAN.R-project.org/package=CircStats>

564 Marques, A. T., Batalha, H., Rodrigues, S., Costa, H., Pereira, M. J. R., Fonseca, C.,

565 Mascarenhas, M., & Bernardino, J. (2014). Understanding bird collisions at wind

566 farms: An updated review on the causes and possible mitigation strategies. *Biological*

567 *Conservation*, 179, 40–52. <https://doi.org/10.1016/j.biocon.2014.08.017>

568 Marques, A. T., Santos, C. D., Hanssen, F., Muñoz, A., Onrubia, A., Wikelski, M., Moreira,

569 F., Palmeirim, J. M., & Silva, J. P. (2020). Wind turbines cause functional habitat loss

570 for migratory soaring birds. *Journal of Animal Ecology*, 89(1), 93–103.

571 <https://doi.org/10.1111/1365-2656.12961>

572 Martin, J., Calenge, C., Quenette, P.-Y., & Allainé, D. (2008). Importance of movement

573 constraints in habitat selection studies. *Ecological Modelling*, 213(2), 257–262.

574 <https://doi.org/10.1016/j.ecolmodel.2007.12.002>

575 Martin-Díaz, P., Cortés-Avizanda, A., Serrano, D., Arrondo, E., Sánchez-Zapata, J. A., &

576 Donázar, J. A. (2020). Rewilding processes shape the use of Mediterranean

577 landscapes by an avian top scavenger. *Scientific Reports*, 10(1), Article 1.

578 <https://doi.org/10.1038/s41598-020-59591-2>

579 May, R. F. (2015). A unifying framework for the underlying mechanisms of avian avoidance
580 of wind turbines. *Biological Conservation*, 190, 179–187.
581 <https://doi.org/10.1016/j.biocon.2015.06.004>

582 McClure, C. J. W., Rolek, B. W., Dunn, L., McCabe, J. D., Martinson, L., & Katzner, T.
583 (2021). Eagle fatalities are reduced by automated curtailment of wind turbines.
584 *Journal of Applied Ecology*, 58(3), 446–452. <https://doi.org/10.1111/1365-2664.13831>

585 Monserrat, S., Benhamou, S., Sarrazin, F., Bessa-Gomes, C., Bouter, W., & Duriez, O.
586 (2013). How Predictability of Feeding Patches Affects Home Range and Foraging
587 Habitat Selection in Avian Social Scavengers? *PLOS ONE*, 8(1), e53077.
588 <https://doi.org/10.1371/journal.pone.0053077>

589 Nathan, R., Spiegel, O., Fortmann-Roe, S., Harel, R., Wikelski, M., & Getz, W. M. (2012).
590 Using tri-axial acceleration data to identify behavioral modes of free-ranging animals:
591 General concepts and tools illustrated for griffon vultures. *Journal of Experimental
592 Biology*, 215(6), 986–996. <https://doi.org/10.1242/jeb.058602>

593 Pennycuick, C. J. (1998). Field Observations of Thermals and Thermal Streets, and the
594 Theory of Cross-Country Soaring Flight. *Journal of Avian Biology*, 29(1), 33–43.
595 <https://doi.org/10.2307/3677338>

596 Pennycuick, C. J. (2008). *Modelling the Flying Bird*. Elsevier.

597 Péron, G., Fleming, C. H., Calabrese, J. M., Duriez, O., Fluhr, J., Itty, C., Lambertucci, S. A.,
598 Safi, K., & Shepard, E. L. (2017). The energy landscape predicts flight height and
599 wind turbine collision hazard in three species of large soaring raptor. *Journal of
600 Applied Ecology*, 54, 1895–1906. <https://doi.org/10.1111/1365-2664.12909>

601 Perrow, M. (2017). *Wildlife and Wind Farms - Conflicts and Solutions: Onshore: Potential
602 Effects*. Pelagic Publishing Ltd.

603 Plonczkier, P., & Simms, I. C. (2012). Radar monitoring of migrating pink-footed geese:
604 Behavioural responses to offshore wind farm development. *Journal of Applied
605 Ecology*, 49(5), 1187–1194. <https://doi.org/10.1111/j.1365-2664.2012.02181.x>

607 R Core Team. (2022). *R: A language and environment for statistical computing. R*
608 *Foundation for Statistical Computing, Vienna, Austria.* [Computer software].
609 <https://www.R-project.org/>

610 Santos, C. D., Ramesh, H., Ferraz, R., Franco, A. M. A., & Wikelski, M. (2022). Factors
611 influencing wind turbine avoidance behaviour of a migrating soaring bird. *Scientific*
612 *Reports*, 12(1), Article 1. <https://doi.org/10.1038/s41598-022-10295-9>

613 Scacco, M., Arrondo, E., Donázar, J. A., Flack, A., Sánchez-Zapata, J. A., Duriez, O.,
614 Wikelski, M., & Safi, K. (2023). The species-specificity of energy landscapes for
615 soaring birds, and its consequences for transferring suitability models across
616 species. *Landscape Ecology*, 38(1), 239–252. <https://doi.org/10.1007/s10980-022-01551-4>

618 Schaub, T., Klaassen, R. H. G., Bouteren, W., Schlaich, A. E., & Koks, B. J. (2020). Collision
619 risk of Montagu's Harriers *Circus pygargus* with wind turbines derived from high-
620 resolution GPS tracking. *Ibis*, 162(2), 520–534. <https://doi.org/10.1111/ibi.12788>

621 Schuster, E., Bulling, L., & Köppel, J. (2015). Consolidating the State of Knowledge: A
622 Synoptical Review of Wind Energy's Wildlife Effects. *Environmental Management*,
623 56(2), 300–331. <https://doi.org/10.1007/s00267-015-0501-5>

624 Shepard, E. L. C. (2022). Energy economy in flight. *Current Biology*, 32(12), R672–R675.
625 <https://doi.org/10.1016/j.cub.2022.02.004>

626 Signer, J., Fieberg, J., & Avgar, T. (2019). Animal movement tools (amt): R package for
627 managing tracking data and conducting habitat selection analyses. *Ecology and*
628 *Evolution*, 9(2), 880–890. <https://doi.org/10.1002/ece3.4823>

629 Tang, W., & Bennett, D. A. (2010). Agent-based Modeling of Animal Movement: A Review.
630 *Geography Compass*, 4(7), 682–700. <https://doi.org/10.1111/j.1749-8198.2010.00337.x>

632 Thaxter, C. B., Buchanan, G. M., Carr, J., Butchart, S. H. M., Newbold, T., Green, R. E.,
633 Tobias, J. A., Foden, W. B., O'Brien, S., & Pearce-Higgins, J. W. (2017). Bird and bat

634 species' global vulnerability to collision mortality at wind farms revealed through a
635 trait-based assessment. *Proceedings of the Royal Society B: Biological Sciences*,
636 284(1862), 20170829. <https://doi.org/10.1098/rspb.2017.0829>

637 Tomé, R., Canário, F., Leitão, A. H., Pires, N., & Repas, M. (2017). Radar Assisted
638 Shutdown on Demand Ensures Zero Soaring Bird Mortality at a Wind Farm Located
639 in a Migratory Flyway. In J. Köppel (Ed.), *Wind Energy and Wildlife Interactions: Presentations from the CWW2015 Conference* (pp. 119–133). Springer International
640 Publishing. https://doi.org/10.1007/978-3-319-51272-3_7

641 Williams, H. J., Duriez, O., Holton, M. D., Dell'Omo, G., Wilson, R. P., & Shepard, E. L. C.
642 (2018). Vultures respond to challenges of near-ground thermal soaring by varying
643 bank angle. *The Journal of Experimental Biology*, 221(23), jeb174995.
644 <https://doi.org/10.1242/jeb.174995>
645